Dynamics of a Gyroscope

Francesco Mascadri

May 31 2020

Contents

List of Figures

1 Introduction

In this report, a gyroscope is modelled and analysed using Newton-Euler equations to describe the system and then solving these equations in MATLAB. The objective of this report is to explore and characterise the behaviour of the gyroscope, with particular focus on the gyroscopic effect and precession.

A gyroscope is a spinning rotor where the spin axis is free to move. Gyroscopes are often mounted in gimbals which give additional degrees of freedom to the system. The orientation of the spin axis is not affected by rotational motion of the mounting. Because of this consistent spin axis alignment when rotating, gyroscopes are often used as rotation sensors in inertial navigation systems and accelerometers.

The underlying principle of the gyroscope's motion is illustrated in Figure 1. A gyroscope rotor is shown in Figure 1a. There is a positive rotation of ω about the z-axis. This rotation has an angular momentum, L_1 along the z-axis. If the gyroscope is placed on a stand off the ground as in Figure 1b, the weight force mg acts at a distance r from the contact point. This weight force creates a torque, τ_2 about the y-axis. This positive rotation about the y-axis from τ_2 then has angular momentum L_2 in the negative y-direction as can be seen in Figure 1c. The resultant angular momentum L_R of L_1 and L_2 causes the whole system to rotate. Provided that ω is sufficiently large, the gyroscope system can continue to rotate without falling.

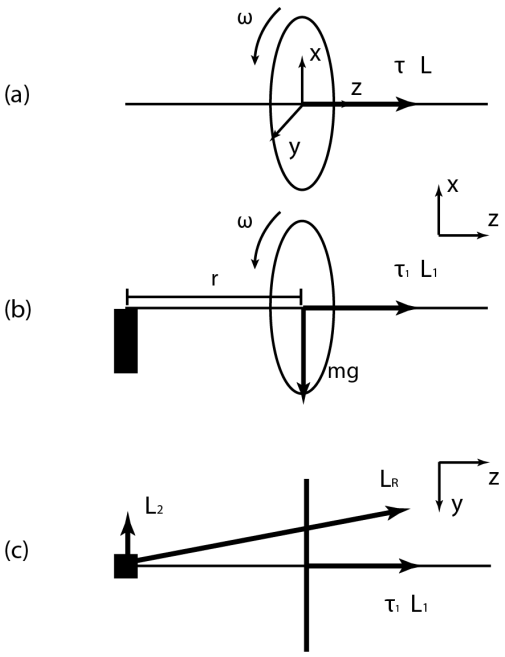

Figure 1: Illustration of gyroscopic effect

The gyroscope analysed in this report is a toy gyroscope which is composed of a frame with a narrow point connecting to the ground, a rotor which spins within the frame and is wound with a pull-string to give the rotor an initial angular velocity. Figure 2 shows the gyroscope studied in this report.

Figure 2: Toy gyroscope under analysis

2 Modelling

In this section the gyroscope system is modelled, the equations of motion are calculated and the system is simulated. The calculations are performed in MATLAB (see GitHub repo) and most of the intermediate matrix values in the calculations are omitted in this section for brevity. The initial modelling in this section uses estimated parameters. The estimates of the geometry and mass parameters as well as the initial conditions are further refined in the following section.

2.1 Defining rotation matrices

The frames of the system are defined as in Figure 3 and the rotation matrices between these frames are:

The rotation from frame $\{0\}$ to frame $\{1\}$ is a negative rotation about the y_0 axis.

$$ {}^{0}_{1}R = \begin{bmatrix} \cos(\alpha) & 0 & -\sin(\alpha) \\ 0 & 1 & 0 \\ \sin(\alpha) & 0 & \cos(\alpha) \end{bmatrix} $$

The rotation from frame $\{1\}$ to frame $\{2\}$ is a positive rotation about the x_1 axis.

$$ {}^{1}_{2}R = \begin{bmatrix} 1 & 0 & 0 \\ 0 & \cos(\beta) & -\sin(\beta) \\ 0 & \sin(\beta) & \cos(\beta) \end{bmatrix} $$

The rotation from frame $\{2\}$ to frame $\{3\}$ is a positive rotation about the z_2 axis.

$$ {}^{2}_{3}R = \begin{bmatrix} \cos(\gamma) & -\sin(\gamma) & 0 \\ \sin(\gamma) & \cos(\gamma) & 0 \\ 0 & 0 & 1 \end{bmatrix} $$

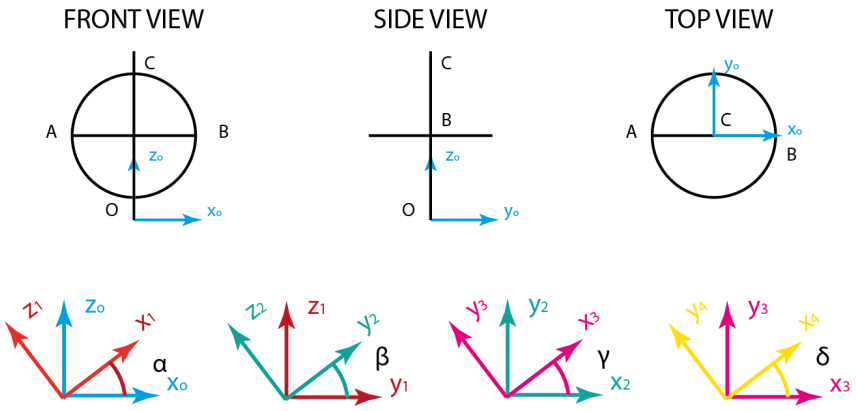

Figure 3: Frames associated with the gyroscope

The rotation from frame {3} to frame {4} is a positive rotation about the z_3 axis.

$$ {}^3_4R = \begin{bmatrix} \cos(\delta) & -\sin(\delta) & 0 \\ \sin(\delta) & \cos(\delta) & 0 \\ 0 & 0 & 1 \end{bmatrix} $$

2.2 Defining tensors of inertia

The tensors of inertia for the gyroscope frame and the rotor are defined in this section. The tensor of inertia for the frame is composed of three components for each of the three bodies that make up the frame: the thin rod, the x-z torus and the x-y torus.

The tensor of inertia for the rod in frame {3}, ${}^3I^G_{rod}$, about the centre of the mass of the frame G, is

$$ {}^3I^G_{rod} = m_1 \begin{bmatrix} \frac{3*r^2+H^2}{12} & 0 & 0 \\ 0 & \frac{3*r^2+H^2}{12} & 0 \\ 0 & 0 & \frac{r^2}{2} \end{bmatrix} $$

The tensor of inertia for the torus in frame {3} with axes of symmetry x-z, ${}^3I^G_{xz}$, about the centre of mass of the frame G, is

$$ {}^3I^G_{xz-torus} = m_2 \begin{bmatrix} \frac{5r^2}{8} + \frac{R_o^2}{2} & 0 & 0 \\ 0 & \frac{3r^2}{4} + R_o^2 & 0 \\ 0 & 0 & \frac{5r^2}{8} + \frac{R_o^2}{2} \end{bmatrix} $$

The tensor of inertia in frame {3} for the torus with axes of symmetry x-y, ${}^3I^G_{xy}$, about the centre of mass of the frame G, is

$$ {}^3I^G_{xy-torus} = m_3 \begin{bmatrix} \frac{5r^2}{8} + \frac{R_o^2}{2} & 0 & 0 \\ 0 & \frac{5r^2}{8} + \frac{R_o^2}{2} & 0 \\ 0 & 0 & \frac{3r^2}{4} + R_o^2 \end{bmatrix} $$

By superposition principle, these tensors may be added to give the tensor of inertia for the whole frame,

$$ {}^3I^G_{frame} = {}^3I^G_{rod} + {}^3I^G_{xz-torus} + {}^3I^G_{xy-torus} $$

The rotor is modelled as a cylinder rather than a torus. For this specific toy gyroscope, either approach would appear valid however the cylinder was chosen to capture the mass of the bearing and decorative wire mesh about the attachment point. The tensor of inertia for the rotor is:

$$ {}^4I^G_{rotor} = m_4 \begin{bmatrix} \frac{3R_i^2+h^2}{12} & 0 & 0 \\ 0 & \frac{3R_i^2+h^2}{12} & 0 \\ 0 & 0 & \frac{R_i^2}{2} \end{bmatrix} $$

2.3 Defining gravity forces

The weight forces for each body are defined in their respective frames:

$$ {}^3G_{frame} = \begin{bmatrix} 0 \\ 0 \\ -(m_1+m_2+m_3)g \end{bmatrix} $$

$$ {}^4G_{rotor} = \begin{bmatrix} 0 \\ 0 \\ -m_4 g \end{bmatrix} $$

Transforming each of these to frame {0} gives,

$$ {}^0G_{frame} = {}^0_1R^1_2R^2_3R^3G_{frame} $$

$$ {}^0G_{rotor} = {}^0_1R^1_2R^2_3R^3_4R^4G_{rotor} $$

2.4 Kinematic quantities

The linear and angular velocities and accelerations for each body are developed here.

2.4.1 Kinematic quantities of the frame

Angular velocity of frame {1},

$$ {}^1\omega_1 = \begin{bmatrix} 0 \\ -\dot{\alpha} \\ 0 \end{bmatrix} $$

The relative velocity of frame {2} relative to frame {1} is,

$$ {}^2\omega_{21} = \begin{bmatrix} \dot{\beta} \\ 0 \\ 0 \end{bmatrix} $$

The relative angular velocity of frame {3} relative to frame {2} is

$$ {}^3\omega_{32} = \begin{bmatrix} 0 \\ 0 \\ \dot{\gamma} \end{bmatrix} $$

The absolute angular velocity of the gyroscope frame represented in frame {3} is,

$$^{3}\omega_3 = {}^{3}_{2}R^{2}_{1}R^{1}\omega_1 + {}^{3}_{2}R^{2}\omega_{21} + {}^{3}\omega_{32}$$

The absolute angular acceleration of the gyroscope frame represented in frame {3} is,

$$^{3}\dot{\omega}_3 = {}^{3}\omega_3'$$

The linear velocity and acceleration of the gyroscope frame represented in frame {3} is,

$$^{3}r_{OG_f} = \begin{bmatrix} 0 \\ 0 \\ L \end{bmatrix}$$

$$^{3}\dot{r}_{OG_f} = {}^{3}r_{OG_f}{}' + {}^{3}\omega_3 \times {}^{3}r_{OG_f}$$
$$^{3}\ddot{r}_{OG_f} = {}^{3}\dot{r}_{OG_f}{}' + {}^{3}\omega_3 \times {}^{3}\dot{r}_{OG_f}$$

2.4.2 Kinematic quantities of rotor

The linear and angular velocity of the rotor is developed here.

The relative angular velocity and acceleration of rotor relative to the gyroscope frame are,

$$^{4}\omega_{43} = \begin{bmatrix} 0 \\ 0 \\ \dot{\delta} \end{bmatrix}$$

$$^{4}\dot{\omega}_{43} = \begin{bmatrix} 0 \\ 0 \\ \ddot{\delta} \end{bmatrix}$$

The absolute angular velocity and acceleration of the rotor expressed in frame {4} are,

$$^{4}\omega_4 = {}^{4}_{3}R^{3}\omega_3 + {}^{4}\omega_{43}$$

$$^{4}\dot{\omega}_4 = {}^{4}_{3}R^{4}\dot{\omega}_4 + {}^{4}\omega_{43} + {}^{4}_{3}R^{3}\omega_3 \times {}^{4}\omega_{43}$$

The linear velocity and acceleration of the centre of mass of the rotor G_r represented in frame {4} are,

$$^{4}r_{OG_r} = \begin{bmatrix} 0 \\ 0 \\ L \end{bmatrix}$$

$$^{4}\dot{r}_{OG_r} = {}^{4}r_{OG_r}{}' + {}^{4}\omega_4 \times {}^{4}r_{OG_r}$$
$$^{4}\ddot{r}_{OG_r} = {}^{4}\dot{r}_{OG_r}{}' + {}^{4}\omega_4 \times {}^{4}\dot{r}_{OG_r}$$

2.5 Newton-Euler equations

From the rotation matrices, weight forces and other kinematic quantities found previously, the Newton-Euler equations of the system are developed beginning with the rotor.

The 'linear' portion of the Newton-Euler equations starting from the rotor is,

$$^4F_4 = m_4 {}^4\ddot{r}_{OG_r} - {}^4_0R^0G_{rotor}$$

The 'angular' portion of the Newton-Euler equations for the rotor is,

$$^4M_4 = {}^4r_{OG_r} \times {}^4F_4 + {}^4I^G_{rotor}{}^4\dot{\omega}_4 + {}^4\omega_4 \times ({}^4I^G_{rotor}{}^4\omega_4)$$

From these results for the rotor, the linear portion of the Newton-Euler equations for the gyroscope frame is,

$$^3F_3 = (m_1 + m_2 + m_3){}^3\ddot{r}_{OG_f} + {}^3_4R^4F_4 - {}^3_0R^0G_{frame}$$

And, the angular portion is,

$$^3M_3 = {}^3_4R^4M_4 + {}^3r_{OG_f} \times {}^3F_3 + {}^3r_{OG_f} \times ({}^3_4R^4F_4){}^3I^G_{frame}{}^3\dot{\omega}_3 + {}^3\omega_3 \times ({}^3I^G_{frame}{}^3\omega_3)$$

2.6 Reduce to independent equations

The Newton-Euler equation results from the prior section are of the general form,

$$^kF_k = \begin{bmatrix} {}^kF_{k,x} \\ {}^kF_{k,y} \\ {}^kF_{k,z} \end{bmatrix}$$

$$^kM_k = \begin{bmatrix} {}^kM_{k,x} \\ {}^kM_{k,y} \\ {}^kM_{k,z} \end{bmatrix}$$

where $^4F_4$ is the force applied by the gyroscope frame on the rotor at point G represented in frame $\{4\}$,

$$^4F_4 = \begin{bmatrix} {}^4F_{4,x} \\ {}^4F_{4,y} \\ {}^4F_{4,z} \end{bmatrix}$$

and $^4M_4$ is the moment acting on the rotor from the gyroscope frame at point G represented in frame $\{4\}$, where the $\tau_{rotor,z}$ component is the torque in the z-direction from the rotation of the rotor.

$$^4M_4 = \begin{bmatrix} {}^4M_{4,x} \\ {}^4M_{4,y} \\ \tau_{rotor,z} \end{bmatrix}$$

$^3F_3$ is the force applied by the ground on the gyroscope at point O represented in frame $\{4\}$,

$$^3F_3 = \begin{bmatrix} {}^3F_{3,x} \\ {}^3F_{3,y} \\ {}^3F_{3,z} \end{bmatrix}$$

and ${}^3M_3$ is the moment acting on the gyroscope frame from the ground at point O represented in frame {4}, where the components are the torques in the three axial directions about the spherical 'joint' at point O.

$$ {}^3M_3 = \begin{bmatrix} \tau_{frame,x} \\ \tau_{frame,y} \\ \tau_{frame,z} \end{bmatrix} $$

These four independent moments are extracted as the four equations of motion for the system and are brought into the form,

$$ \begin{bmatrix} \tau_{rotor,z} \\ \tau_{frame,x} \\ \tau_{frame,y} \\ \tau_{frame,z} \end{bmatrix} = \begin{bmatrix} g_1(\alpha,\beta,\gamma,\delta,\dot{\alpha},\dot{\beta},\dot{\gamma},\dot{\delta},\ddot{\alpha},\ddot{\beta},\ddot{\gamma},\ddot{\delta}) \\ g_2(\alpha,\beta,\gamma,\delta,\dot{\alpha},\dot{\beta},\dot{\gamma},\dot{\delta},\ddot{\alpha},\ddot{\beta},\ddot{\gamma},\ddot{\delta}) \\ g_3(\alpha,\beta,\gamma,\delta,\dot{\alpha},\dot{\beta},\dot{\gamma},\dot{\delta},\ddot{\alpha},\ddot{\beta},\ddot{\gamma},\ddot{\delta}) \\ g_4(\alpha,\beta,\gamma,\delta,\dot{\alpha},\dot{\beta},\dot{\gamma},\dot{\delta},\ddot{\alpha},\ddot{\beta},\ddot{\gamma},\ddot{\delta}) \end{bmatrix} $$

2.7 Decouple equations of motion

These four equations of motion are linear in $\ddot{\alpha}$, $\ddot{\beta}$, $\ddot{\gamma}$ and $\ddot{\delta}$. With this linearity, the equations are decoupled using MATLAB into the form,

$$ \begin{bmatrix} \ddot{\alpha} \\ \ddot{\beta} \\ \ddot{\gamma} \\ \ddot{\delta} \end{bmatrix} = \begin{bmatrix} h_1(\alpha,\beta,\gamma,\delta,\dot{\alpha},\dot{\beta},\dot{\gamma},\dot{\delta}) \\ h_2(\alpha,\beta,\gamma,\delta,\dot{\alpha},\dot{\beta},\dot{\gamma},\dot{\delta}) \\ h_3(\alpha,\beta,\gamma,\delta,\dot{\alpha},\dot{\beta},\dot{\gamma},\dot{\delta}) \\ h_4(\alpha,\beta,\gamma,\delta,\dot{\alpha},\dot{\beta},\dot{\gamma},\dot{\delta}) \end{bmatrix} $$

2.8 Simulation and Animation

These decoupled equations were converted into state space form and solved using ode45 in MATLAB. After creating the 3D surfaces and objects, the results of the simulation were plotted. Figures 4 and 5 show the initial test configuration plots of the gyroscope model with fixed values of the angles.

The results of the simulation from the ODE solver were then animated using this gyroscope model and videos of different modes of operation with different parameters and initial conditions were produced.

3 Choosing Parameter Values and Initial Conditions

The geometric and mass parameters for this model of the gyroscope system were taken from the lab materials unless otherwise noted.

3.0.1 Geometric parameters

- Cross-sectional radius of frame components, r=2mm
- Height of cylindrical rod, H=8mm. The provided measurement was smaller but in this model of the system the rod extends all the wall from point O to point C.
- Height of the rotor, h = 7mm
- Major radius of frame torus, R_o = 35mm

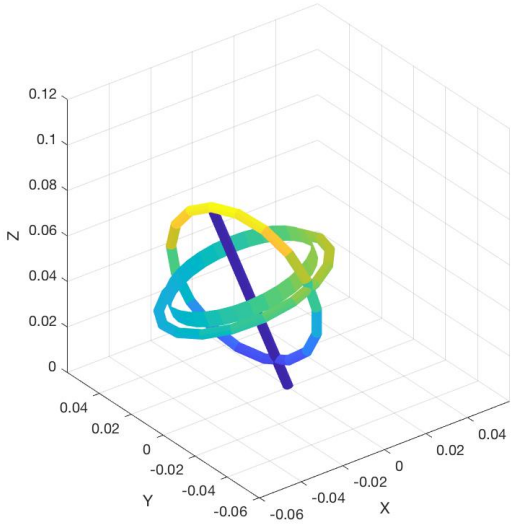

Figure 4: Initial plot of the gyroscope model with α and γ at 15° and β at $-15°$

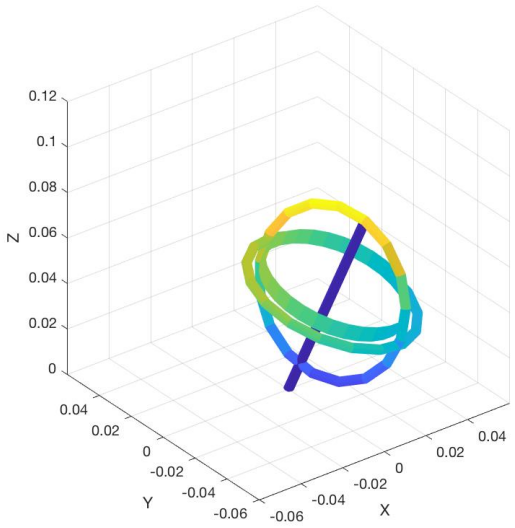

Figure 5: Initial plot of the gyroscope model with α at $-15°$ and β and β at 15°

- Radius of rotor, $R_i = 30$mm. This was given in the lab materials as 34mm however a smaller radius was selected to aid in visibility of the rotor in the animation.
- Distance from point O to point G, $L = 47$mm.

3.0.2 Mass parameters

- Mass of cylindrical rod, $m_1 = 20$g
- Mass of xz torus, $m_2 = 11.5$g
- Mass of xy torus, $m_3 = 11.5$g
- Mass of rotor, $m_4 = 45$g

The mass of the entire frame was given in the lab materials, so the total mass was divided as above to the individual components of the frame.

3.0.3 Initial conditions

The initial conditions were selected iteratively. The first attempt was for initial conditions:

$$\begin{bmatrix} \alpha_0 \\ \beta_0 \\ \gamma_0 \\ \delta_0 \\ \dot{\alpha_0} \\ \dot{\beta_0} \\ \dot{\gamma_0} \\ \dot{\delta_0} \end{bmatrix} = \begin{bmatrix} 0 \\ 0 \\ 0 \\ 0 \\ 0 \\ 0 \\ 0 \\ 40 \end{bmatrix}$$

However this resulted in a vertical, balanced gyroscope while the rotor spun. This did not match the observations from the lab demonstration and it was unreasonable to assume that the gyroscope would be placed perfectly vertical on point O. The next attempt was for initial conditions where,

$$\begin{bmatrix} \alpha_0 \\ \beta_0 \\ \gamma_0 \\ \delta_0 \\ \dot{\alpha_0} \\ \dot{\beta_0} \\ \dot{\gamma_0} \\ \dot{\delta_0} \end{bmatrix} = \begin{bmatrix} 5^\circ \\ 5^\circ \\ 5^\circ \\ 0 \\ -10deg/sec \\ 10deg/sec \\ 10deg/sec \\ 2300deg/sec \end{bmatrix}$$

This allowed for a reasonable disturbance in the placement of the gyroscope on point O with small angles about point O and angular velocities.

From this stage, various initial rotor angular velocities, , were trialled to see the effects of faster and slower rotor spin. When faster initial rotor angular velocities were trialled, the observed precession was tighter than when the angular velocity was slower.

4 Analysis

In this section, the results of the simulation are compared to the observed real-life gyroscope motion and the provided simulation videos for the lab.

Figures 6, 7, 8 and 9 show isometric, front, side and top views of the initial configuration of the gyroscope at t=0. These are taken from the attached animated videos of the gyroscope's motion. In

these animations, there are a few differences noted between the simulation and animation and the provided videos in the lab.

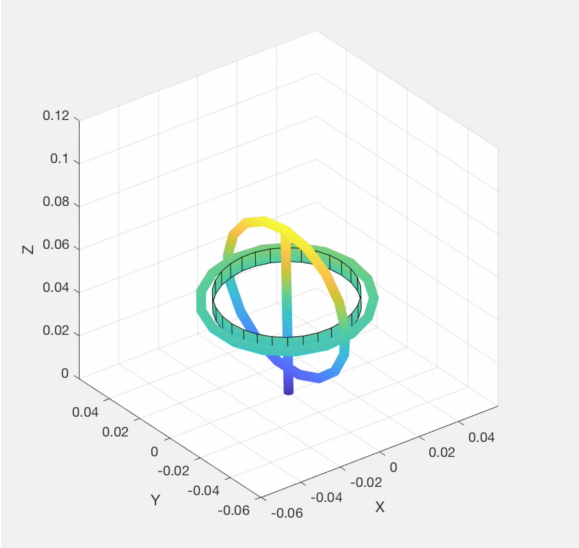

Figure 6: Isometric view of gyroscope at $\dot{\delta_0} = 60$ rad/s

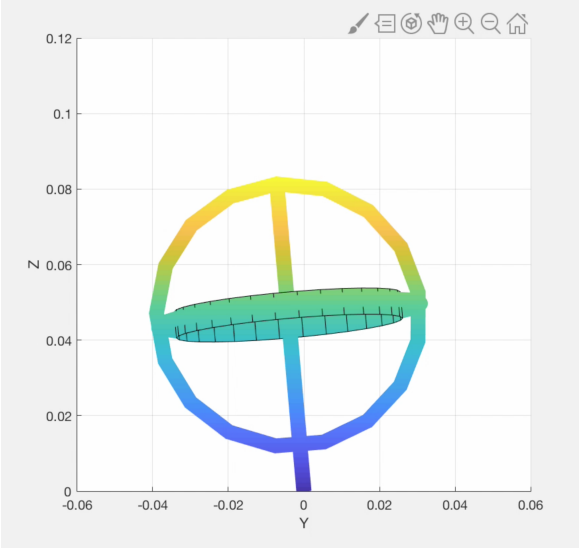

Figure 7: Front view of gyroscope at $\dot{\delta_0} = 60$ rad/s

The simulation animations successfully show the rotation of the rotor and gyroscope's precession about the point O. At high initial rotor velocities, the precession is tight about the starting configuration. At sufficiently low initial rotor speeds, the gyroscope rotor does not have a large enough angular momentum to remain upright and the gyroscope simply falls.

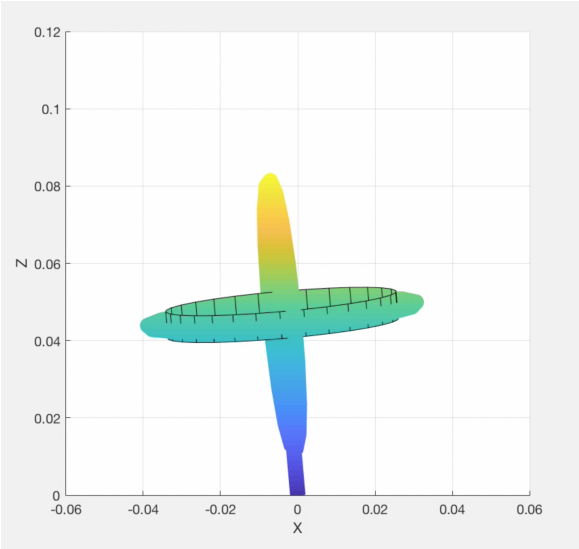

Figure 8: Side view of gyroscope at $\dot{\delta_0} = 60$ rad/s

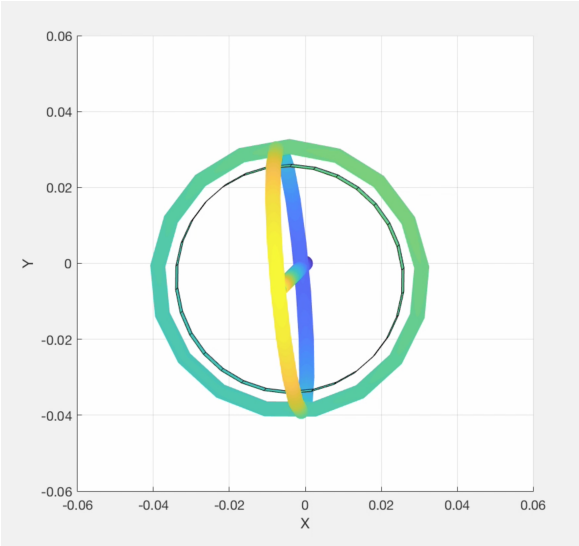

Figure 9: Top view of gyroscope at $\dot{\delta_0} = 60$ rad/s

The most noticeable difference between the model here and real-world observations is the lack of rotation of the gyroscope frame driven by the rotor bearing friction. In this modelling and analysis work, friction was ignored. The friction in the connection between the rotor and the frame slows the rotor down but it also imparts a torque to the frame at the contact point. This causes a rotation of the frame itself in the same direction as the rotation of the rotor.

5 Concluding Remarks

In this report, the toy gyroscope system was successfully modelled, simulated and analysed. Further work could be done to capture the effects of friction on the system.